Discrimination of gamma rays due to inelastic neutron scattering in AGATA

A. Ataç[*,a], A. Kaşkaş[a], S. Akkoyun[a,1], M. Şenyiğit[a], T. Hüyük[a], S. O. Kara[a], J. Nyberg[b]

[a]*Department of Physics, Faculty of Science, Ankara University, 06100 Tandoğan, Ankara, Turkey*
[b]*Department of Physics and Astronomy, Uppsala University, SE-75121 Uppsala, Sweden*

Abstract

Possibilities of discriminating neutrons and γ rays in the AGATA γ-ray tracking spectrometer have been investigated with the aim of reducing the background due to inelastic scattering of neutrons in the high-purity germanium crystals. This background may become a serious problem especially in experiments with neutron-rich radioactive ion beams. Simulations using the GEANT4 toolkit and a tracking program based on the forward tracking algorithm were carried out by emitting neutrons and γ rays from the center of AGATA. Three different methods were developed and tested in order to find "fingerprints" of the neutron interaction points in the detectors. In a simulation with simultaneous emission of six neutrons with energies in the range 1-5 MeV and ten γ rays with energies between 150 and 1450 keV, the peak-to-background ratio at a γ-ray energy of 1.0 MeV was improved by a factor of 2.4 after neutron rejection with a reduction of the photopeak efficiency at 1.0 MeV of only a factor of 1.25.

Key words: Gamma-ray tracking, AGATA, HPGe detectors, neutron-gamma discrimination, inelastic neutron scattering, GEANT4 Monte Carlo simulations
PACS: 29.40.Mc, 29.85.Ca

1. Introduction

One of the large challenges of contemporary experimental nuclear structure physics is to study exotic nuclides, which lie far from the line of β stability. For production of such proton- and neutron-rich nuclei the usage of radioactive ion beams is essential. The intensity of such beams is, however, several orders of magnitude lower than what is obtainable with stable beams and the production rates of the exotic nuclides are very low. In order to partly compensate for the low production rates highly efficient detection techniques are being developed. One such technique is γ-ray tracking [1]. Two γ-ray tracking arrays made of segmented high-purity germanium (HPGe) detectors are currently under development, AGATA [2] in Europe and GRETA [3] in the USA. These future instruments promise an increase in performance over existing detector arrays by several orders of magnitude for certain experimental conditions. This increase in the experimental sensitivity opens up

the opportunity to study very weak reaction channels and interesting nuclear phenomena.

One of the most common types of nuclear reactions used in nuclear structure physics is the heavy-ion fusion-evaporation (HIFE) reaction in which two nuclei fuse to form a compound nucleus that decays by evaporating a number of light particles, mainly neutrons, protons, and/or α particles. In contrast to the light charged particles, neutrons can travel long distances and interact within the germanium detectors together with the γ rays emitted by the residual nuclei. Neutrons are detected indirectly in AGATA either via elastic scattering with the Ge nuclei or via nuclear reactions which may produce neutrons, charged particles and γ rays. Elastic scattering, $^{nat}Ge(n,n)^{nat}Ge$, gives the largest contribution to the total cross-section in the neutron energy range of interest for HIFE reactions, from about 1 to 10 MeV, while inelastic scattering, $^{nat}Ge(n,n'\gamma)^{nat}Ge$, has the second largest cross section in this energy range [4]. The expected probability of neutrons with energies 1-10 MeV to be detected by AGATA is about 50 %, if the low-energy threshold of the Ge detector signals is set to 5 keV (target value for AGATA) [5].

In several recent articles [4, 5, 6, 7], experimental studies of neutron interactions in segmented HPGe

---

[*]Corresponding author
Email addresses: `atac@science.ankara.edu.tr` (A. Ataç), `johan.nyberg@physics.uu.se` (J. Nyberg)
[1]Present address: Cumhuriyet Üniversitesi, 58140, Campus Sivas, Turkey

detectors were reported with the aim of reducing the neutron-induced background in the γ-ray spectra and to utilize segmented HPGe detector arrays to measure neutrons. In an earlier Monte Carlo simulation [5] of the AGATA γ-ray spectrometer, the background in the γ-ray spectra due to the inelastic scattering of neutrons was discussed and different possibilities of background suppression were investigated without any conclusive results. The neutron background is expected to become a serious problem in future studies, especially when using neutron-rich radioactive ion beams of the coming facilities, e.g. NUSTAR/FAIR [8, 9], and SPIRAL2 [10], and in experiments where a low background in the γ-ray spectra is of importance.

In this work, a GEANT4 [11] based Monte Carlo simulation of the AGATA spectrometer [12] has been performed in order to investigate the possibility of reducing the neutron induced background by γ-ray tracking. The tracking algorithm of the mgt program [13, 14] has been used to identify the neutron interaction points and methods for eliminating the γ rays originated from inelastic neutron scattering have been developed with a special emphasis on not reducing the photopeak (= full-energy peak) efficiency of the γ rays of interest.

An obvious method of distinguishing between neutrons and γ rays is to use the time-of-flight technique. This possibility was previously investigated in a simulation of the AGATA array [4]. It is still an open question if the time resolution that can be achieved by using pulse-shape analysis with segmented HPGe detectors will be sufficient to discriminate neutrons from γ rays. The time-of-flight technique may be a complementary procedure that can be used together with the tracking based methods presented in this work.

2. Monte Carlo simulations and γ ray tracking

The interaction points of neutrons and γ rays in the HPGe detectors of AGATA were simulated with the GEANT4 toolkit versions 4.9.0 and 4.9.2 using the neutron cross section data libraries G4NDL3.11 and G4NDL3.13, respectively. Within the low-energy models of neutron scattering used by GEANT4 prior to version 4.9.2, errors related to the angular distribution of scattered neutrons as well as errors in the energy distribution of the scattered neutrons, of the recoiling nuclei, and of the γ rays produced after the inelastic scattering of neutrons, were reported on the GEANT4 problem tracking system [15]. In version 4.9.2 of GEANT4 these bugs have been corrected. In our work we used for GEANT4 version 4.9.0 a modification of the GEANT4 code that was suggested by J. Ljungvall et al. [4] and which corrects

for the errors in the energy distribution of the germanium recoils. We noted that our results regarding inelastic scattering of 1 to 5 MeV neutrons on germanium obtained by GEANT4 version 4.9.0, with the correction suggested by J. Ljungvall et al. [4] were similar to the ones obtained with GEANT4 version 4.9.2.

The full AGATA array with 180 HPGe crystals was used in the GEANT4 simulations. The AGATA HPGe detectors were arranged in a 4π geometry around the central source position (= target position in an in-beam experiment). In most of the simulations presented in this work only the HPGe crystals (no other material) were included. In a few of the simulations, the aluminium capsules in which the HPGe crystals are mounted, were also included.

In a typical HIFE reaction the majority of the neutrons are emitted in the energy range 1-5 MeV with a high-energy tail that extends up to about 15 MeV. In this work we either simulated the emission of mono-energetic neutrons or neutrons with a flat energy distribution from 1 to 5 MeV, which covers the majority of the neutrons emitted in a HIFE reaction.

The recoil energies of the Ge ions are not fully converted into electron-hole pairs. This gives rise to the pulse-height defect (PHD) [16] that was included in the simulations as suggested in ref. [4]. The Ge ionization energy E_I is expressed as

$$E_I = a \cdot E_R^b, \quad a = 0.21, \quad b = 1.099, \quad (1)$$

where E_R is the Ge recoil energy in the HPGe crystal.

The output of the GEANT4 simulation program that contains the energy and three-dimensional position of each of the interaction points in AGATA was used as input to the mgt γ-ray tracking program. At this stage mgt has no information whether the interaction is due to a γ ray or a neutron. Thus, the neutron interactions are treated in the same way as the γ-ray interactions during the tracking process.

Before applying the tracking with mgt the interaction points that are located closer to each other than 5 mm were packed together. Their energies were summed and their new position was calculated as the energy-weighted average position. The packed interaction energies were smeared by a Gaussian distribution with a full-width-at-half-maximum (FWHM) corresponding to the typical intrinsic resolution of a large volume HPGe detector. The interaction positions were then smeared by a Gaussian distribution having a FWHM of 5 mm at 100 keV. The smearing parameter had an energy dependence of (interaction point energy)$^{-1/2}$. Interaction points that have an energy lower than a threshold energy

of 5 keV were removed. The selection of this value is based on measured [17] low-energy thresholds of the actual AGATA HPGe detectors. For accepting an event in AGATA the deposited energy in at least one crystal must be larger than about 30 to 50 keV. Such a trigger condition was tested and it was found that it had a negligible effect on the discrimination of events due to inelastic scattering of neutrons. Therefore, only the 5 keV energy threshold was used in this work.

The `mgt` code uses a forward tracking method which is developed by several groups in Europe[14, 18] and in the USA [19]. The method is based on the clusterization of interaction points belonging to the same initial photon. The clusters contain interaction points with a limited angular range, which is a result of the forward peaked Compton-scattering cross section and the fast decrease of the mean free path in Ge as the γ ray looses its energy. An interaction is allowed to be a member of several clusters since at the end of the tracking only the cluster with the lowest figure-of-merit (FM) value is accepted. The FM calculation is based on a comparison of the energy of the scattered γ rays calculated by using the interaction energies and by applying the Compton scattering formula to the positions of the interaction points. The probabilities for Compton scattering, pair production, and photo absorption (photoelectric effect), as well as the probability for the γ ray to travel the distances between the interaction points in a cluster, are also included in the FM.

As an example, the equation for the FM of a cluster with two interaction points, the first one due to a Compton scattering and the second one due to photo absorption, is given by

$$FM = \left(\frac{E_{\gamma,1}(\text{en}) - E_{\gamma,1}(\text{pos})}{E_{\gamma,0}}\right)^2 \cdot$$
$$\frac{d\sigma_{\text{KN}}/d\Omega}{P_{\text{Comp}}(E_{\gamma,0})P(r_1)P_{\text{photo}}(E_{\gamma,1})P(r_2)}. \quad (2)$$

Here $E_{\gamma,1}(\text{en})$ is the energy of the scattered γ ray after the first interaction point

$$E_{\gamma,1}(\text{en}) = E_{\gamma,0} - E_1, \quad (3)$$

with $E_{\gamma,0}$ being the sum of all interaction points (= incident energy for a fully absorbed and correctly tracked γ ray) and E_1 the energy deposited at the first interaction point. $E_{\gamma,1}(\text{pos})$ is also the energy of the scattered γ ray after the first interaction point, but calculated by using the Compton formula

$$E_{\gamma,1}(\text{pos}) = E_{\gamma,0}\left[1 + \frac{E_{\gamma,0}(1 - \cos\theta)}{m_e c^2}\right]^{-1}, \quad (4)$$

where the scattering angle of the γ ray, θ, is calculated by using the position coordinates of the three interaction points (target position, first and second interaction points in this example) and $m_e c^2$ is the rest mass of the electron. The probabilities for traveling the distances r_1 and r_2 are given by

$$P_\lambda(r_1) = e^{-r_1/\lambda(E_{\gamma,0})}, \quad P_\lambda(r_2) = e^{-r_2/\lambda(E_{\gamma,1})}, \quad (5)$$

where λ is the mean free path of γ rays in Ge. The probabilities for Compton scattering and photo absorption are given by

$$P_{\text{Comp}} = \frac{\sigma_{\text{Comp}}(E_{\gamma,0})}{\sigma_{\text{tot}}(E_{\gamma,0})},$$
$$P_{\text{photo}} = \frac{\sigma_{\text{photo}}(E_{\gamma,1}(\text{en}))}{\sigma_{\text{tot}}(E_{\gamma,1}(\text{en}))}. \quad (6)$$

The differential cross section $d\sigma_{\text{KN}}/d\Omega$, which does not have an important effect on our tracking results, is the Klein-Nishina Compton scattering cross section for unpolarized radiation.

During the tracking process the FM values of all possible permutations of interaction points are evaluated. The one with the lowest FM value is chosen as an accepted tracked γ ray, but only of its FM value is < 1. It should be noted that similar but not identical FM definitions as in eq. 2 are given in refs. [18, 19]. These three FM equations are implemented as options in `mgt` and they give similar results [17].

The properties of the data sets used in this work are summarized in table 1. Data sets 1, 4, and 5 were produced in order to develop the methods for the discrimination of neutron and γ-ray interaction points. Data set 6 contains events produced with a flat distribution of neutron energies from 1 to 5 MeV, which well enough emulates the energy distribution of neutrons emitted in a typical HIFE reaction. The results obtained with data set 6 were compared to the ones obtained with data set 2, which contains events generated by 1 MeV γ rays emitted from the center of AGATA. The energy 1 MeV was chosen to represent a typical average γ-ray energy. Finally, a more realistic simulation was carried out with a flat distribution of neutron energies between 1 and 5 MeV emitted from the center of AGATA together with a γ-ray cascade representing a "rotational band" populated after a HIFE reaction, data set 7. The results obtained with data set 7 were compared to the results of data set 3, which does not contain any neutron emissions.

3

Table 1: Energies and multiplicities of γ rays and neutrons in the simulated data sets used in this work. The Ge isotope enrichment and the used pulse-height defect (PHD) correction are also given. The γ-ray cascade is a "rotational band" with 10 transitions from E_γ = 150 keV to 1450 keV with ΔE_γ = 150 keV.

Data set number	Ge enrichment	γ-rays		neutrons		PHD
		E_γ [keV]	M_γ	E_{n} [MeV]	M_{n}	
1	^{74}Ge	596	1	-	0	-
2	$^{\mathrm{nat}}$Ge	1000	1	-	0	-
3	$^{\mathrm{nat}}$Ge	cascade	10	-	0	-
4	^{74}Ge	-	0	1	1	no
5	^{74}Ge	-	0	1, 3, 5	1	yes
6	$^{\mathrm{nat}}$Ge	-	0	1-5	1	yes
7	$^{\mathrm{nat}}$Ge	cascade	10	1-5	6	yes

3. Ge recoil energy distributions

The n + $^{\mathrm{nat}}$Ge reaction cross section is more or less constant for neutron energies in the range 1-5 MeV and it is dominated by elastic scattering [4]. Inelastic scattering has the second largest cross section, being a factor of 8 and 1.3 smaller than elastic scattering at the neutron energies 1 MeV and 5 MeV, respectively. In this energy interval the cross sections of other reactions are much smaller and have in the context of this work been neglected. In the elastic scattering process, some of the neutron energy is deposited in the detector via the recoiling Ge nuclei. These energies give rise to single-hit clusters during the γ-ray tracking process and they are mostly eliminated from the data since their FM value is not good enough and they do not qualify as photo-absorption points. Inelastic scattering of neutrons is more complicated since in this case the recoiling Ge nuclei usually also emit γ rays. These γ rays cause an unwanted background in the γ-ray spectra.

Simulations of the Ge recoil energy distributions were performed by using the most recent version of GEANT4 (version 4.9.2). Distributions for the different Ge isotopes as well as for $^{\mathrm{nat}}$Ge were investigated. The shapes of the recoil energy distributions are determined by the fairly isotropic angular distributions and by the reaction kinematics. For scattering of 1 MeV neutrons on $^{\mathrm{nat}}$Ge, the recoil energy extends from 0 to 57 keV for elastic scattering. The recoil energy distributions due to inelastic scattering of 1 to 5 MeV neutrons on $^{\mathrm{nat}}$Ge are shown in fig. 1a. The recoil energies due to inelastic scattering of 1 MeV neutrons extends from 0 to about 35 keV for the even-even isotopes ^{70}Ge, ^{72}Ge, ^{74}Ge, and ^{76}Ge and to 53 keV for ^{73}Ge.

Figure 1b shows the effect of the PHD correction (eq. 1) on the recoil energies. The maximum recoil energy

after inelastic neutron scattering with E_{n} = 1 MeV is only 16.7 keV after the PHD correction. With a low-energy threshold of 5 keV, 52 % of the neutron interaction points for 1 MeV neutrons and 5 % for 5 MeV neutrons will not be detected after the PHD correction.
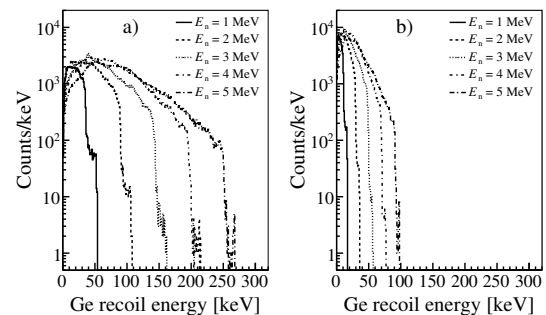

Figure 1: Recoil energies of $^{\mathrm{nat}}$Ge after inelastic scattering of neutrons with energies from 1 to 5 MeV, a) without and b) with PHD correction.

4. Number of interaction points

In a simplified example, we have investigated whether the γ-ray tracking code can discriminate between two types of γ-rays with the same energies, namely 596 keV. The first type of γ ray is emitted from the center of AGATA (data set 1), while the second type is created within a HPGe detector after inelastic scattering of 1 MeV neutrons on ^{74}Ge (data set 4). This is illustrated in the inset of fig. 2. To avoid creating γ rays of other energies than 596 keV from the inelastic neutron scattering, the AGATA HPGe detectors were in this simulation configured to consists only of ^{74}Ge isotopes. With 1 MeV neutrons one can only populate the first excited 2_1^+ state at 596 keV in ^{74}Ge (the second excited

state is at 1204 keV), which then de-excites to the 0_1^+ ground state by emitting a 596 keV γ ray.

The number of interaction points (npt) in ^{74}Ge determined by the tracking algorithm is shown in fig. 2. When the incoming particle is a 1 MeV neutron npt is increased on the average by one unit compared to the events where the incoming particle is a 596 keV γ ray. This increase in the npt value is due to the neutron interaction point that is included in the `mgt` cluster together with the γ-ray interaction points.
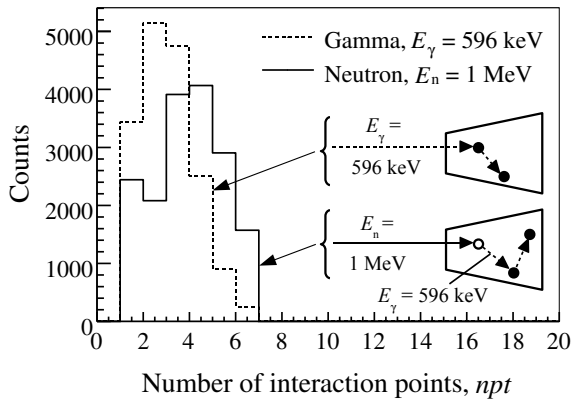

Figure 2: Number of interaction points in ^{74}Ge after tracking. The spectra are normalized to have the same number of counts.

Simulated and tracked γ-ray spectra obtained after inelastic scattering of 1 MeV neutrons on ^{74}Ge are shown for different npt values in fig. 3. Apart from the peak at 596 keV, a bump is visible at higher γ-ray energies. This bump originates from the `mgt` clusters where the interaction point due to the Ge recoil is included in the cluster and its energy is added to 596 keV. As npt increases, it becomes more likely that one of the interaction points is due to the scattering of neutrons and the bump becomes more prominent. At $E_n = 1$ MeV the width of the recoil energy distribution is 35 keV (see section 3). The FWHM of the bump in fig. 3 is about 65 keV for $npt = 6$, which indicates that there may be two or even three neutron interaction points in the clusters, apart from the γ-ray interaction points.

5. Neutron-γiscrimination methods

Based on a comparison of data sets 1 and 4, three methods to distinguish between two types of γ rays, were investigated.
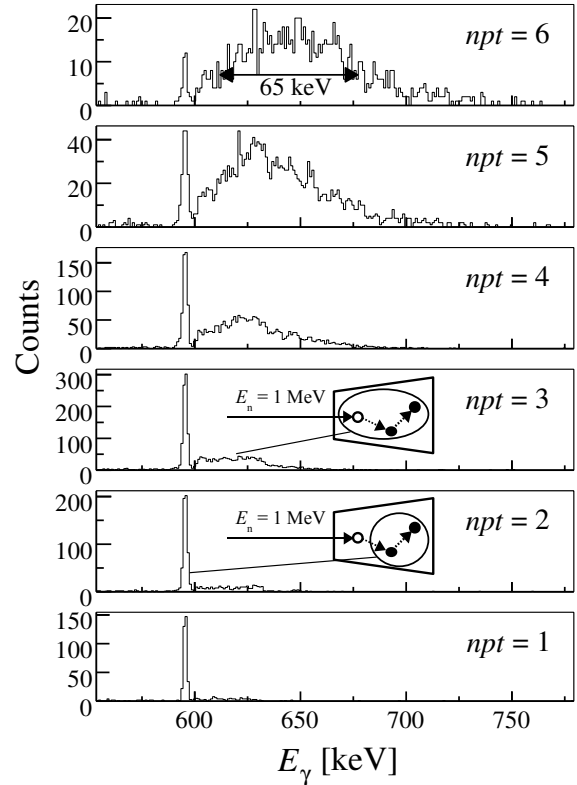

Figure 3: Gamma-ray spectra due to inelastic scattering of 1 MeV neutrons on ^{74}Ge (data set 4) obtained after γ-ray tracking. In sub-figures $npt = 2$ and $npt = 3$, an example with three interactions points is illustrated. The first interaction point is due to the recoiling Ge nucleus after inelastic scattering of the neutron (open circle). The second and third interaction points (filled circles) are due to Compton scattering and photo absorption, respectively, of the γ ray produced in the decay of the excited Ge nucleus. If the neutron interaction point is not measured or not included in the `mgt` cluster, the 596 keV peak in the $npt = 2$ spectrum is incremented. Otherwise, if the recoil energy is measured and included in the cluster, the bump in the $npt = 3$ spectrum is incremented.

5.1. Method 1: Energy deposited in the first and second interaction points

The first method is based on the low energy deposition in the detectors by the recoiling Ge nuclei after inelastic scattering of neutrons. Distributions of the energies of the first (E_1) and second interaction points (E_2) for each `mgt` cluster are shown in fig. 4. For 1 MeV neutrons both the E_1 and E_2 spectra have large abundances of counts at low energies, below about 40 keV, compared to the spectra of 596 keV γ rays emitted from the center of AGATA. With a condition (gate) of E_1 and E_2 to be > 40 keV one can discriminate a large number of the cases in which the incoming particle is a neutron compared to a γ ray. For the second interaction point the shape of the spectrum for incoming 596 keV

γ rays is somewhat different than for the first interaction point, in particular at low energies. With a gate at $E_2 > 40$ keV slightly more of the photopeak efficiency of the 596 keV peak is lost as compared to the same gate on E_1. In the simulations presented below the gate on E_2 was therefore set at a smaller value of the interaction point energy. The energies of the third interaction point were also studied but they were not used for gating in this work since they caused an even bigger loss in the photopeak efficiency than E_2.
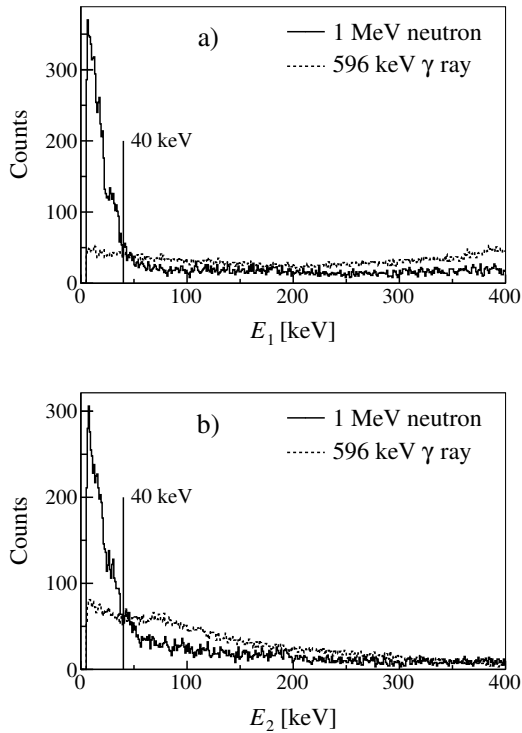

Figure 4: Energy deposited in a) the first and b) the second interaction points. The spectra were obtained by sending 596 keV γ rays (dashed lines, data set 1) and 1 MeV neutrons (solid lines, data set 4) from the center of AGATA. The HPGe detectors were made of ^{74}Ge isotopes in these simulations. The spectra in a) and b) have been normalized to have the same number of counts.

5.2. Method 2: Difference in incoming direction of the γay

The second method is based on the difference in the incoming direction of the initial γ rays. If they come from random positions in space, they must be produced by inelastic neutron scattering in the HPGe detectors. If they come from the center of the array, they are likely not produced by reactions in the detectors. Two different angles, θ_g and θ_c, are extracted and compared in this investigation in a similar way that was used in ref. [5]. As illustrated in fig. 5, θ_g is the geometric angle between the line that goes from the center of the detector array to the first interaction point and the line that connects the first interaction point to the second one. Thus, θ_g is determined from the positions of the interaction points relative to the center of AGATA. The angle θ_c is the scattering angle calculated from the Compton scattering formula using the total energy deposited by the γ ray (sum of all energies in the cluster) and the energy of the first interaction point obtained after γ-ray tracking.
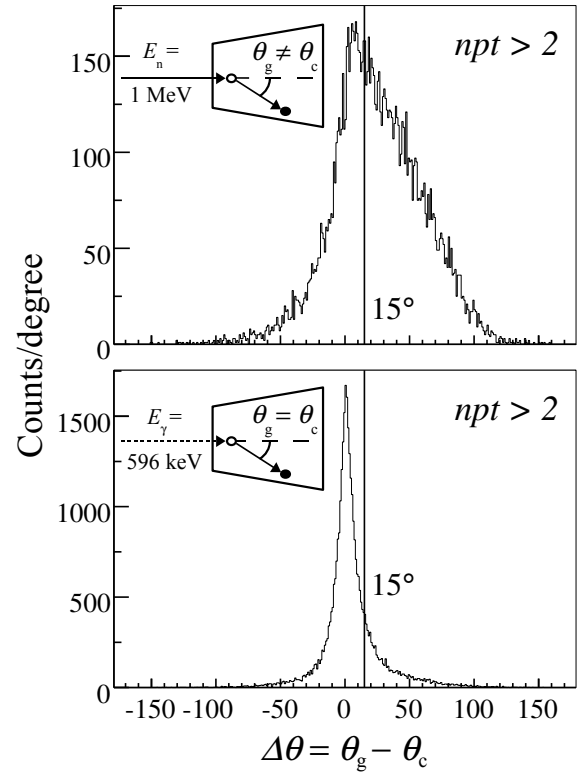

Figure 5: Distribution of the difference $\Delta\theta = \theta_g - \theta_c$ obtained when emitting 596 keV γ rays (lower, data set 1) and 1 MeV neutrons (upper, data set 4) from the center of AGATA. The HPGe detectors were made of ^{74}Ge isotopes in these simulations. The angle θ_g is obtained from the position of the interaction points whereas θ_c is obtained from the Compton scattering formula.

If the γ ray comes from the center of AGATA we have $\theta_g = \theta_c$ and we expect to see a sharp distribution of the difference $\Delta\theta = \theta_g - \theta_c$ centered at 0°. The width of this distributions is due to the errors in the determination of the energy and position of the interaction points. Such a distribution is seen in the lower part of fig. 5. The upper part of the same figure shows the distribution of γ rays produced by inelastic scattering of 1 MeV neutrons on ^{74}Ge. This distribution is wider than the first one and it

6

is asymmetric around 0°. The asymmetry is due to the low-energy interaction points (due to Ge recoils), which are accepted by the tracking code as forward Compton scattered γ rays with a small θ_c angle giving an excess of positive $\Delta\theta$ values. In this work we have used the condition $\Delta\theta > 15°$, in order to discriminate neutrons and γ rays. If $\Delta\theta$ is larger than 15° the cluster is assumed to contain a γ ray from inelastic neutron scattering. It should be mentioned that the neutron rejection obtained by this method can be improved with a better interaction position resolution. An increased position resolution leads to a smaller width of the distribution in the lower part of fig. 5, which allows the use of a lower value of the gate on $\Delta\theta$.

5.3. Method 3: Selection based on the FM value

The third method is based on a comparison of figure-of-merit values (FM) of the clusters determined by the `mgt` tracking algorithm when the initial particles are 1 MeV neutrons and 596 keV γ rays emitted from the center of AGATA. In the `mgt` program a cluster is accepted only if all its interactions are valid as one of the three γ-ray processes: Compton scattering, photo absorption, or pair production. The validity depends on the energies deposited at each interaction point, the probability of the process to happen and the interaction length before the process takes place. A cluster that contains a neutron interaction point may be accepted ($FM < 1$) only if the neutron interaction point accidentally qualifies as a γ-ray interaction point. Such a cluster is, however, expected to give a higher FM value (eq. 2) as compared to a cluster with only γ-ray interactions.

Figure 6 shows a comparison of the FM values of the clusters constructed by the `mgt` code after the emission of 596 keV γ rays from the center of AGATA and the FM values of the clusters constructed after the emission of 1 MeV neutrons. In this figure both "accepted" and "good" γ rays belong to clusters with $FM < 1$. The energy of the "good" γ rays, however, has the value of 596 keV, i.e. it is equal to the incoming γ-ray energy. The FM distribution of the "good" γ rays is strongly peaked at small FM values and it decreases much faster than the distribution due to 1 MeV neutrons. With the help of fig. 6 we decided to use the gate $0.05 < FM < 1$ in order to discriminate between neutrons and γ rays.

6. Comparison of interaction distances

We have also investigated and compared the distances from the center of AGATA to the first interaction point for 596 keV γ rays emitted a) from the center of AGATA
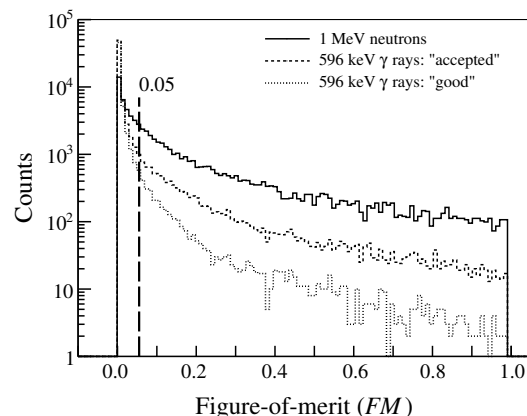

Figure 6: Figure-of-merit (FM) values of the `mgt` code when the initial particles are 596 keV γ rays (dashed lines, data set 1) and 1 MeV neutrons (solid line, data set 4) emitted from the center of AGATA. The HPGe detectors were made of ^{74}Ge isotopes in these simulation. The label "accepted" γ rays indicates the γ rays which fulfill the requirement $FM < 1$, whereas the "good" γ rays in addition have an energy of 596 keV. The histogram of the 1 MeV neutrons and the "accepted" 596 keV γ rays have been normalized to have the same number of counts.

(data set 1) and b) from inelastic scattering of 1 MeV neutrons (data set 4) on ^{74}Ge. The comparison was done both for the real first interaction point as obtained from the Geant4 simulation (before tracking) and for the first interaction point as obtained by `mgt` (after tracking). The results are shown in fig. 7. For 596 keV γ rays emitted from the center of AGATA, the distributions of the distances to the first interaction point before and after tracking are very similar. The centroid of the distribution is at 26 cm, which corresponds to the mean free path of 596 keV γ rays in Ge, 2.5 cm, plus the 23.5 cm distance from the center to the front face of the Ge detectors. For 1 MeV neutrons there is an abundance of events for which the real first interaction distances (before tracking) are well above 26 cm (see fig. 7). However, the events with too large interaction distances are eliminated by `mgt` because the $P_\lambda(r_1)$ value becomes too small, which leads to an FM value larger than 1 (see eqs. 2-5).

We have found that setting different conditions on the interaction distances in `mgt` rejects rather few neutron events and leads to a relatively large loss of photopeak efficiency, compared to what we have achieved with the other three methods mentioned above. Since this is also true for higher neutron energies (up to 5 MeV), it is concluded here that gating on the interaction distances is not beneficial for improving the neutron-γ discrimina-
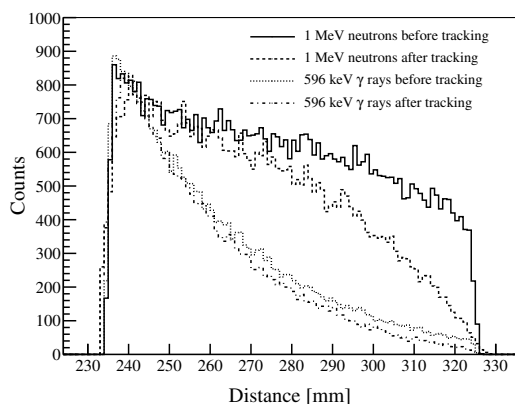
tion.

Figure 7: Interaction distances measured from the center of AGATA to the first interaction point for 596 keV γ rays (data set 1) and for inelastic scattering of 1 MeV neutrons (data set 4) on ^{74}Ge. The histograms have been arbitrarily normalized.

Figure 8: Reduction of the 596 keV peak and its bump after applying different neutron-γ discrimination methods. The spectra were obtained by sending 1 MeV neutrons on ^{74}Ge (data set 4). See caption of table 2 for the definition of the gates I and II.

7. Applications of the neutron-γiscrimination methods

The results of the applications of the different neutron-γ discrimination methods, as described in section 5, are presented in this section.

7.1. 596 keV γays and 1 MeV neutrons (data set 1 and 4)

Fig. 8 shows tracked γ-ray spectra in the region around the 596 keV peak and its bump obtained from events generated by inelastic scattering of 1 MeV neutrons on ^{74}Ge (data set 4). The dashed and dotted lines indicate what is left after applying different gates. Quantitative values of the achieved reductions are shown in table 2 together with the reduction of the photopeak efficiency of the 596 keV peak for 596 keV γ rays emitted from the center of AGATA (data set 1). The aim of the gating is to reduce the 596 keV peak and its bump in the neutron induced spectra as much as possible while keeping the photopeak efficiency of the 596 keV peak in the γ-ray induced spectra as large as possible.

By using gate set II (E_1, E_2, $\Delta\theta$, FM) the total spectrum is reduced by 69 %, the 596 keV transition by 47 % and the bump by 92 % in the 1 MeV neutron induced spectrum. This causes a loss of 22 % in the 596 keV full-energy peak of the spectrum obtained by sending
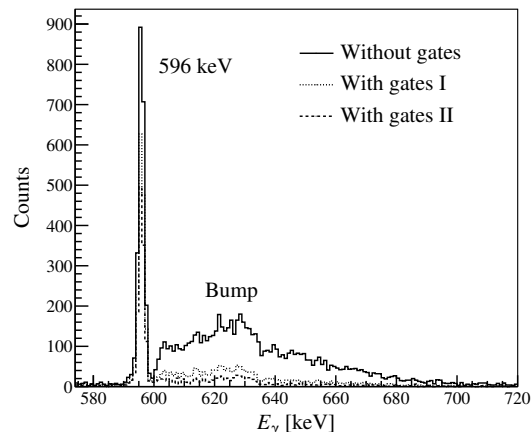
596 keV γ rays form the center of AGATA. The two neutron-γ discrimination methods that contribute least to the reduction of the photopeak efficiency of γ rays emitted from the center of AGATA are the E_1 and FM tests. If we use an or of gates based on these two methods (gate set I) the total neutron induced spectrum is reduced by 58 % while the peak is reduced by 32 % and the bump by 77 %. This causes a loss of 11 % of the 596 keV full-energy peak in the γ-ray induced spectrum.

Note that the three methods for neutron-γ discrimination do not exclude each other and there is an overlap of neutron events rejected by the different gates. For example, the application of gate set I gives a total neutron rejection of 58 %, which is lower than the sum of the results given by the E_1 and FM gates separately. It is a different situation when the same gate set is applied on the 596 keV γ rays emitted from the center of AGATA. In this case there is no overlap of the events rejected by the different methods and the total loss in the full-energy peak is a sum of the losses obtained by the E_1 and FM gates separately, as is seen in the last column of table 2.

7.2. Pulse-height defect correction

The energies of the neutron interaction points are reduced considerably when the PHD correction is included in the simulations, see section 2. If the interaction energy is below the low-energy threshold of 5 keV it will not be measured and the rejection methods, in particular method 1 which uses E_1 (and E_2), will not give as good results as the ones shown in table 2.

8

Table 2: Reduction of counts in percent of the 596 keV peak, its bump, and of the total spectrum after applying different neutron-γ discrimination gates. The results were obtained by sending 1 MeV neutrons (data set 4) and 596 keV γ rays (data set 1) on ^{74}Ge. The gates used were $E_1 < 40$ keV, $E_2 < 30$ keV, $\Delta\theta > 15°$, $0.05 < FM < 1$. The gate combinations (E_1, FM) and $(E_1, E_2, \Delta\theta, FM)$ are labelled I and II, respectively, and were created by using a logical or of the individual gates.

| | 1 MeV neutrons (data set 4) | | | 596 keV γ rays (data set 1) |
Gates	596 keV peak	Bump	Total	Peak
E_1	6	63	40	6
$\Delta\theta$	26	65	46	11
FM	28	55	44	5
I: (E_1, FM)	32	77	58	11
II: $(E_1, E_2, \Delta\theta, FM)$	47	92	69	22

In figs. 9a) and b) the effect of the PHD correction on the γ-ray spectra obtained by inelastic scattering of 1 MeV neutrons on ^{74}Ge is shown (data sets 4 and 5). Apart from the reduced energies one can also observe a reduction of the bump and a corresponding increase of the counts in the 596 keV full-energy peak. This is due to the fact that some counts are moved from the bump to the peak if the recoil energy is not measured. As shown in figs. 9b), c) and d), the bump gets wider and moves to higher energies as the neutron energy increases from 1 MeV to 5 MeV (cf. the recoil energy distributions shown in fig. 1). When the bump moves to higher energies less of the counts in it will be lost due to the 5 keV energy threshold.
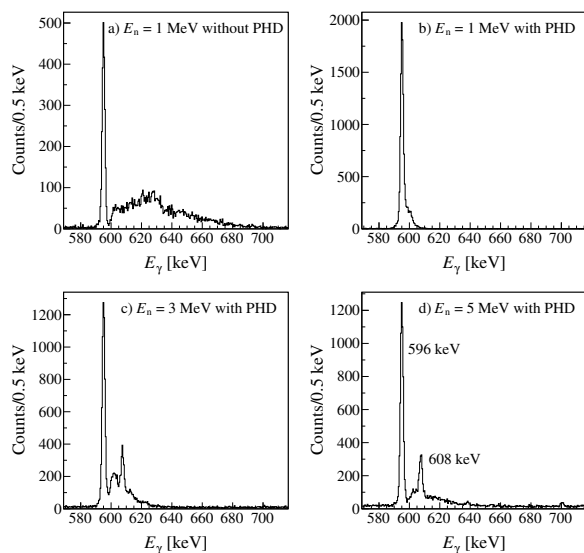

Figure 9: Tracked γ-ray spectra obtained after inelastic scattering of neutrons on ^{74}Ge (data sets 4 and 5). The 596 keV and 608 keV peaks are due to the $2_1^+ \to 0_1^+$ and $2_2^+ \to 2_1^+$ transitions in ^{74}Ge, respectively.

The PHD correction was applied in all simulations presented in the rest of this section.

7.3. 1 MeV γays and 1-5 MeV neutrons (data sets 2 and 6)

In this subsection the results of inelastic scattering of 1-5 MeV neutrons on ^{nat}Ge are presented. The neutrons had a flat energy distribution and the PHD correction was applied (data set 6). The different neutron-γ discrimination methods described in subsection 5 were tested and their effect on the photopeak efficiency was checked by a simulation of 1 MeV γ rays emitted from the center of AGATA (data set 2).

In fig. 10 the histogram with the solid line shows an ungated γ-ray spectrum (no neutron rejection gates were applied) whereas the dotted histogram shows what is left after the application of gate set II (E_1, E_2, $\Delta\theta$, FM). Quantitative results of the application of the different gates are shown in table 3.

With gate set II the total counts in the neutron induced γ-ray spectrum was reduced by 54 %, the 834 keV peak by 39 %, and its bump by 76 % (see table 3). This causes a loss of 14 % of the 1 MeV peak in the spectrum obtained by sending 1 MeV γ rays from the center of AGATA (data set 2). If instead, gate set I is applied, the total neutron induced spectrum is reduced by 40 %, the 834 keV peak by 23 %, and its bump by 58 % whereas the loss in the 1 MeV full-energy peak is only 5 % in the 1 MeV γ-ray induced spectrum.

7.4. Flat energy distribution of 1 to 5 MeV neutrons and a γray cascade (data sets 3 and 7)

In this subsection the results of applying the neutron rejection methods on events in which neutrons are emitted in coincidence with γ rays are presented. A simulation of simultaneous emission of 6 neutrons and a γ-ray cascade of multiplicity 10 (data set 7) was compared

Table 3: Reduction of counts in percent of the 834 keV peak ($2_1^+ \rightarrow 0_1^+$ transition in ^{72}Ge), its bump, and of the total spectrum after applying different neutron-γ discrimination gates. The results were obtained by sending neutrons with a flat energy distribution from 1 to 5 MeV (data set 6) and 1 MeV γ rays (data set 2) on $^{\text{nat}}$Ge. The gates used were $E_1 < 20$ keV, $E_2 < 15$ keV, $\Delta\theta > 15°$, $0.05 < FM < 1$. The gate combinations (E_1, FM) and (E_1, E_2, $\Delta\theta$, FM) are labelled I and II, respectively, and were created by using a logical or of the individual gates.

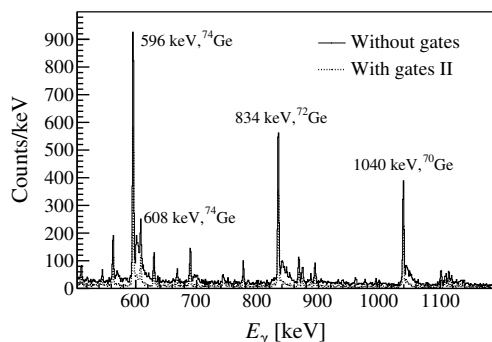| Gates	1-5 MeV neutrons (data set 6)			1 MeV γ rays (data set 2)
	834 keV peak	Bump	Total	Peak
E_1	1	38	11	1
$\Delta\theta$	25	51	36	11
FM	23	45	36	4
I: (E_1, FM)	23	58	40	5
II: (E_1, E_2, $\Delta\theta$, FM)	39	76	54	14

Figure 10: Tracked γ-ray spectra obtained after inelastic scattering of 1-5 MeV neutrons on $^{\text{nat}}$Ge (data set 6). The solid histogram shows the γ-ray spectrum obtained without any neutron rejection gates while the dotted histogram shows what is left after applying gate set II (E_1, E_2, $\Delta\theta$, FM).

to one with no neutron emission (data set 3). The aluminium capsules of the HPGe detectors were included in this simulation. Fig. 11a shows the large and complex background caused by the inelastic scattering of neutrons compared to the spectrum for which no neutrons were emitted.

The influence of the neutrons can be quantified by the peak-to-background ratio (PTB) and the total photopeak efficiency (ϵ) of the γ-ray peaks in the spectra. The results are summarized in tables 4 and 5. The PTB ratio for a γ-ray peak was determined as the number of counts in the peak area divided by the background area, which was defined as a region of $\pm 2\sigma$ around the centroid of the γ-ray peak, with σ being the width of the peak. The two gate sets, I and II, were are used for the neutron-γ discrimination. The ratios of the PTB values, R_{PTB}, which show the improvement of the PTB values when applying the neutron rejection gates I and II on the data set with $M_n = 6$, are also given in the table. The ratios
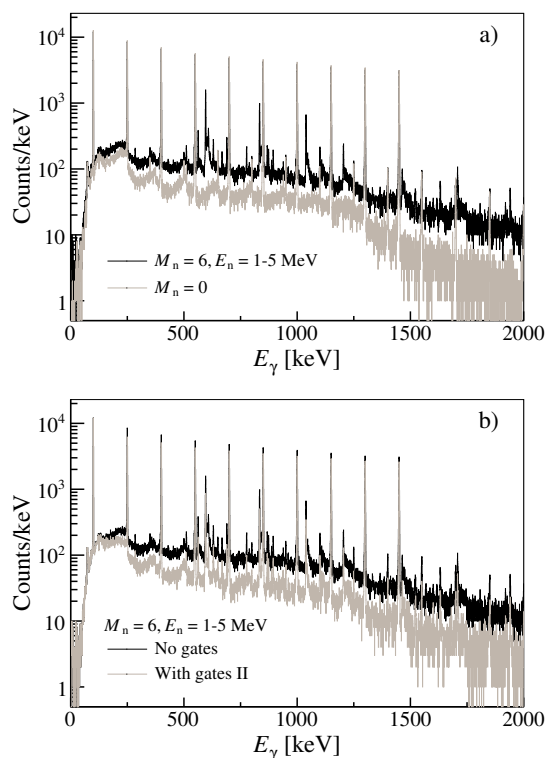

Figure 11: a) Tracked spectrum for a γ-ray cascade of multiplicity 10 when no neutrons are present in the events (gray, data set 3) and when 6 neutrons are emitted in coincidence with the γ rays (black, data set 7). b) Tracked energy of the same γ-ray cascade of multiplicity 10 emitted in coincidence with 6 neutrons before (black) and after (gray) neutron rejection.

R_{PTB} are also plotted as a function of the γ-ray energy in fig. 12a.

As seen in figs. 11a and b, the neutron emission as well as the neutron rejection method has a major influence on the PTB ratios. On the average, the emission of 6 neutrons reduces the PTB ratio by a factor of 2.6,

Table 4: Peak-to-background ratios (PTB) for the emission of 0 and 6 neutrons in coincidence with a γ-ray cascade of multiplicity 10 (data sets 2 and 7). The R_{PTB} values are ratios of the PTB ratios extracted from the gated and ungated spectra with $M_n = 6$ using gate set I (column 4/column 3) and II (column 5/column 3). See caption of table 3 for a description of gates I and II.

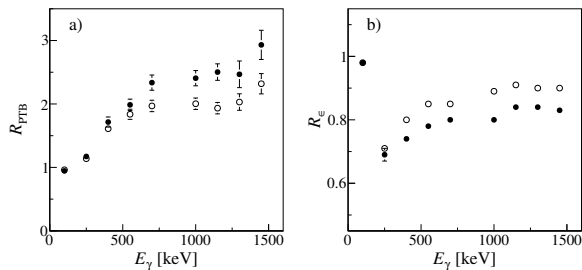| E_γ | Peak-to-background ratio, PTB | | | | R_{PTB} | |
| | No gates | No gates | Gates I | Gates II | I | II |
	$M_n = 0$	$M_n = 6$	$M_n = 6$	$M_n = 6$		
100	32.0	25.2	23.3	23.6	0.93	0.94
250	16.6	10.9	12.0	12.8	1.10	1.17
400	34.6	15.5	24.3	26.5	1.57	1.71
550	36.5	15.3	27.6	30.3	1.80	1.98
700	35.7	15.4	29.7	35.9	1.93	2.33
850	35.8	8.3	17.9	22.1	2.15	2.65
1000	37.5	13.7	26.9	32.8	1.97	2.40
1150	35.4	13.7	26.0	34.3	1.89	2.50
1300	57.2	18.7	40.1	49.5	2.00	2.46
1450	110.2	25.0	56.9	73.2	2.28	2.93

Figure 12: Ratio of a) peak-to-background values R_{PTB} and b) photopeak efficiencies R_ϵ with and without neutron rejection for $M_n = 6$. Open and filled circles were obtained by using gate set I and II, respectively. The data point for the 850 keV γ ray was excluded from the plots because it is located on the bump of the 834 keV transition (see fig. 10) and therefore difficult to analyze.

whereas the neutron rejection method increases it by a factor 1.8 and 2.1 for gates I and II, respectively. At a γ-ray energy of 1 MeV, the PTB ratio is improved from 13.7 to 32.8, i.e. by a factor of 2.4 for gates II. The PTB ratio at 1 MeV is 37.5 for a simulation with no emitted neutrons ($M_n = 0$).

The influence of the neutron emission and of the neutron rejection methods on the photopeak efficiency was also investigated. The emission of neutrons have a negligible influence on the photopeak efficiency. This can be seen by comparing the ϵ values for $M_n = 6$ to the once obtained for $M_n = 0$ in table 5. The neutron rejection, however, decreases the ϵ values. On the average, ϵ is reduced by a factor of 1.16 and 1.24 for the neu-

tron rejection gates I and II, respectively. The R_ϵ values plotted in fig. 12b are the ratios of the ϵ values with and without neutron rejection for gates I and II and $M_n = 6$.

By using gate set II, the photopeak efficiency of the γ-ray peak at 1 MeV was reduced by a factor of 1.25 (20 %) while the ϵ value of the 1039 keV peak, due to the $2_1^+ \rightarrow 0_1^+$ transition in ^{70}Ge, was reduced by a factor of 2.02 (51 %). With gate set I the ϵ value of the γ-ray peak at 1 MeV was reduced by a factor of 1.13 (11 %) and the 1039 keV by a factor of 1.57 (36 %).

A test of the dependency of the R_{PTB} and R_ϵ ratios on the low-energy threshold was also performed. At a γ-ray energy of 1 MeV and with gates II the R_{PTB} was reduced from 2.4 with an energy threshold of 5 keV to 1.9 with a threshold of 30 keV. The R_ϵ value was not effected by the energy threshold.

8. Summary and conclusions

Monte Carlo simulations of neutrons interacting with the HPGe detectors of the AGATA spectrometer were performed. The possibility of using γ-ray tracking for discrimination of interactions due to inelastic scattering of neutrons on Ge was investigated with the aim to suppress the neutron induced background in the γ-ray spectra. Three methods were developed to find "fingerprints" of the neutron interaction points in the detectors and to use them for neutron rejection. The first method makes use of the low Ge recoil energies deposited in the detectors by the scattered neutrons. The second method utilizes the random incoming direction of the initial γ

Table 5: Photopeak efficiency (ϵ) for the emission of 0 and 6 neutrons in coincidence with a γ-ray cascade of multiplicity 10 (data sets 2 and 7). The R_ϵ values are ratios of the photopeak efficiencies extracted from the gated and ungated spectra with $M_\text{n} = 6$ using gate set I (column 4/column 3) and II (column 5/column 3). See caption of table 3 for a description of gates I and II.

| E_γ | Photopeak efficiency, ϵ | | | | R_ϵ | |
| | No gates | No gates | Gates I | Gates II | I | II |
	$M_\text{n} = 0$	$M_\text{n} = 6$	$M_\text{n} = 6$	$M_\text{n} = 6$		
100	0.60	0.57	0.56	0.56	0.98	0.98
250	0.52	0.49	0.35	0.34	0.71	0.69
400	0.48	0.46	0.37	0.34	0.80	0.74
550	0.44	0.41	0.35	0.32	0.85	0.78
700	0.41	0.39	0.33	0.31	0.85	0.80
850	0.38	0.36	0.32	0.29	0.89	0.81
1000	0.37	0.35	0.31	0.28	0.89	0.80
1150	0.35	0.32	0.29	0.27	0.91	0.84
1300	0.23	0.31	0.28	0.26	0.90	0.84
1450	0.31	0.30	0.27	0.25	0.90	0.83

rays that are produced by inelastic neutron scattering. The third method makes use of differences in the figure-of-merit values evaluated by the γ-ray tracking program for γ-ray and neutron induced interactions. These methods were first tested on a simplified case in which neutrons with energies 1 to 5 MeV and multiplicity 1 were emitted from the center of the AGATA spectrometer. With a combination of the three neutron-γ discrimination methods, the 834 keV transition in ^{72}Ge was reduced by 39 % whereas the bump structure that belongs to this transition was reduced more effectively, by 76 %. The bump originates from the tracking of clusters where the Ge recoil energy is added to the energy of the γ ray produced by inelastic scattering of the neutron. The neutron rejection methods were also tested on a case where 6 neutrons with energies between 1 to 5 MeV were emitted in coincidence with a cascade of 10 γ rays. The influence of the neutron emission and the neutron rejection methods were quantified by determining the peak-to-background ratios and total photopeak efficiencies of the γ-ray peaks in the tracked spectra. As a result, two sets of gates, which are combinations of the three neutron rejection methods, were suggested and used. At a γ-ray energy of 1 MeV, the first gate set increases the peak-to-background value by a factor of 2.0, whereas the second set of gates increases it by a factor of 2.4. The same gates reduce the photopeak efficiency at 1 MeV by a factor of 1.13 and 1.25, respectively. The future plan is to test the neutron-γ discrimination methods on real data obtained by the AGATA spectrometer. Neutron-γ discrimination is also important for measure-

ments of high-energy γ rays e.g. from the decay of giant resonances at high temperatures [20]. For this purpose it is necessary to investigate neutron interactions in the energy interval between 5 to 20 MeV. This work is on-going.

References

[1] I.Y. Lee, Nucl. Instr. and Meth. A 422 (1999) 195.
[2] AGATA web site: http://www.gsi.de/agata/.
[3] GRETA web site: http://greta.lbl.gov/.
[4] J. Ljungvall and J. Nyberg, Nucl. Instr. and Meth. A 546 (2005) 553.
[5] J. Ljungvall and J. Nyberg, Nucl. Instr. and Meth. A 550 (2005) 379.
[6] I. Abt et al., Eur. Phys. J. A 36 (2008) 139.
[7] D.G. Jenkins et al., Nucl. Instr. and Meth. (2009), in print.
[8] B. Rubio and T. Nilsson, Nucl. Phys. News 16 (1) (2006) 9.
[9] T. Auman, Prog. Part. Nucl. Phys. 59 (2007) S3.
[10] S. Gales, Prog. Part. Nucl. Phys. 59 (2007) S22.
[11] J. Allison et al., Nucl. Instr. and Meth. A 506 (2003) 250, http://www.geant4.org/.
[12] E. Farnea and D. Bazzacco, LNL Annual Report 2003, p. 158, LNL-INFN(REP)-202/2004, ISBN 88-7337-004-7, see also http://agata.pd.infn.it/.
[13] D. Bazzacco, Nucl. Phys. A 746 (2004) S248c.

[14] D. Bazzacco, unpublished code, developed within the EU TMR network project "Development of γ-ray tracking detectors".
[15] GEANT4 problem tracking system: `http://bugzilla-geant4.kek.jp/`.
[16] G. Knoll, Radiation Detection and Measurements, 3rd Edition, Wiley, 1999.
[17] D. Bazzacco, private communications.
[18] A. Lopez-Martens et al., Nucl. Instr. and Meth. A 533 (2004) 454.
[19] G.J. Schmid et al., Nucl. Instr. and Meth. A 430 (1999) 69.
[20] O. Wieland et al., Phys. Rev. Lett. 97 (2006) 012501.